Eur Biophys J (2008) 37:1157–1165
DOI 10.1007/s00249-008-0279-y

ORIGINAL PAPER

Use of normal modes for structural modeling of proteins: the case study of rat heme oxygenase 1

Jean-Didier Maréchal · David Perahia

Received: 8 October 2007 / Revised: 18 January 2008 / Accepted: 22 January 2008 / Published online: 20 February 2008

Abstract We present an original approach based on full-atom normal mode analysis (NMA) aimed to expand the general framework of homology modeling. Using the rat heme-free oxygenase 1 as a case system, we show how NMA can be used to model different physiologically relevant conformations of the same protein. Starting from a unique heme-bound X-ray structure, and using two structural templates corresponding to a human and an incomplete rat heme-free structures, we generate models of the rat unbound species with open and closed conformations. Less than 100 lowest frequency modes of the target were sufficient to obtain the heme-free conformations, the closest to the templates. The rat HO-1 model built for the open form shows features similar to the open form of the human heme-free oxygenase, and the one built for the closed form was similar to the incompletely resolved X-ray structure of the same protein available in the Protein DataBank. In the latter case, the use of NMA was particularly useful since it allowed to build a complete structure and therefore to discuss on the reason of the structural differences between open and closed forms. This study shows that the amount of main chain flexibility provided by the normal modes can lead to major improvements in homology modeling approaches. Such applications will allow the characterization of alternative conformations of a target protein with respect to the templates and/or the construction of good quality 3D models based on existing templates with unresolved parts in their tertiary structure.

Keywords Normal mode analysis · 3D models · Heme oxygenase · Conformational search · Homology modeling

Regional Biophysics Conference of the National Biophysical Societies of Austria, Croatia, Hungary, Italy, Serbia, and Slovenia.

J.-D. Maréchal (✉)
Unitat de Química Física, Departament de Química, Universitat Autònoma de Barcelona, 08193 Bellaterra, Catalonia, Spain
e-mail: jeandidier.marechal@uab.es

D. Perahia
Laboratoire de Modélisation et d'Ingénierie des Protéines, Institut de Biochimie et Biophysique Moléculaire et Cellulaire d'Orsay, Bât 430, Université Paris-Sud, 91405 Orsay, France

Introduction

Normal mode analysis (NMA) is increasingly applied for characterizing the specific large amplitude motions of macromolecules (Brooks et al. 1995). These types of movements represent highly collective displacements and correspond to slow dynamic events such as domain motions (Guilbert et al. 1996) or more complicated ones such as those observed in multimeric proteins (Thomas et al. 1996; Cui et al. 2004). These motions correspond to the lowest frequency normal modes which describe displacements on the potential energy surface along directions presenting the wider curvatures. However, these motions are often difficult to characterize by standard molecular dynamics simulations, and NMA represents an interesting alternative in this field.

Despite the harmonic approximation that conditions NMA, this method proved very powerful not only to characterize the large amplitude motions in macromolecules but also to isolate metastable or intermediate structures on the potential energy surface (Mouawad and Perahia 1996; Cui and Bahar 2006). At present although a limited number of attempts have been undertaken to apply NMA in this direction; such applications addressed key structural biology

questions like the study of protein folding (Wu et al. 2005), refinement of crystallographic data (Chen et al. 2007), fitting of a high-resolution structure into the cryo-electron microscopy map (Tama et al. 2004), or the generation of structures of relevant interest for dockings whether for small ligands (Cavasotto et al. 2005; Floquet et al. 2006) or protein partners (May and Zacharias 2005). It has also been shown that the structural differences between homologous proteins correspond to collective deformations along combinations of low frequency modes (Leo-Macias et al. 2005). However, to our knowledge, no application of the NMA-based techniques has been done in the general framework of homology modeling—meaning the search of possible alternative conformations of proteins based on structural templates.

Normal mode analysis is based on the diagonalization of the Hessian matrix (matrix of the second derivatives of the potential energy function with respect to the mass weighted coordinates) and takes full advantage of the topology of the potential energy surface around a minimum energy point. Since its size is $3\,N \times 3\,N$, with N the number of atoms, the Hessian matrix can be extremely large for a macromolecule, in particular when one considers explicitly all the atoms of the system. However, significant developments have been achieved in this field allowing the characterization of full-atom normal modes for large macromolecules. Among the existing diagonalization approaches, we can mention iterative methods giving exact results to a given threshold such as that based on diagonalizations in a mixed basis developed in our group (Perahia and Mouawad 1995) and implemented within the CHARMM program (Brooks et al. 1983). Other methods such as block normal mode diagonalization (BNM) (Tama et al. 2000; Li and Cui 2002) or elastic network approaches (Eyal et al. 2006) that use a lower number of degrees of freedom, although very efficient, either ignore or underestimate the flexibility of the side-chains, or do not consider them at all, and therefore may not be appropriate for a fine structural modeling study. Moreover, moderately high-frequency modes (those beyond the third lower frequency ones) influence local arrangements that are better described by a full-atom NMA.

Homology modeling techniques are mainly used to construct a hypothetical structure of a protein of interest (the target) for which only the sequence is known based on the structural features of one or several close parents (the templates). Their general procedure can be summarized as a multi-step process involving: (1) the generation of a series of possible main chain skeletons of the target based on backbone overlaps between the templates; (2) multiple minimization procedure involving side chains and loop optimization; and (3) post-modeling processes aimed to relax the 3D model (MD, minimization in vacuum or solvent, etc.) (Krieger et al. 2003; Eswar et al. 2003). The application of homology modeling approaches has lead to many successes in structural biology and medicinal chemistry, and allowed, in between others, to characterize possible hit compounds for pharmaceutical targets with no 3D structure available in the Protein Data Bank. Still, in some cases, homology modeling studies remain quite challenging. For instance, the initial 3D models generated by homology modeling approaches remain structurally very close to the structure of the templates and rarely present large backbone differences with respect to the templates. Indeed, since the conformational space of the 3D model is directly dependent on the conformational variability of the templates required for the homology modeling process, the conformational sampling remains quite limited. Another problem appears when parts of the tertiary structure are missing in the templates. Generally, for generating the structure of these parts of the protein, different hints are provided by experimental or theoretical approaches (NMR data, secondary structure predictions, etc.) and translated into structural restraints during the homology modeling process (helical restraints, distance restraints between atoms, etc.) (Krieger et al. 2003; Eswar et al. 2003). This latest point is of great deal of interest since numerous protein structures deposited in the Protein Data Bank have parts of the tertiary structure missing. Providing homology modeling techniques with a wider conformational exploration of the backbone is an important topic those days as it is already shown by the variety of algorithms developed for the modeling of the loops (Fiser and Sali 2003).

One interesting example from the literature is the understanding of the conformational variability of mammalian heme oxygenases 1 (HO-1). Heme oxygenases 1 are small (32 kDa) all alpha proteins that perform the first step of the chemical degradation of the heme group; the initial step in HO-1 molecular mechanism is the fixation of the heme group to its binding site. The analysis of the crystal structure of heme-bound HO-1 shows that the heme-HO1 complex is stabilized first by polar interactions between the propionates of the heme and different residues of the apoprotein (Arg183 from the G helix, Tyr134 of the F helix and, in some structures, Lys18 of the A helix), second by a coordination bond between the iron and the His25 from the A helix (Fig. 1). At present two apo forms (heme-free) of HO-1 are available in the Protein Data Bank. One of them is the human heme-free HO-1, which presents an open conformation with the heme-binding site accessible (pdb code 1ni6) (Lad et al. 2003), the other is the heme-free rat HO-1, which presents a closed conformation with a limited access to the heme-binding pocket (pdb code 1irm) (Sugishima et al. 2002) (Fig. 2). Human and rat heme oxygenase 1 species are closely related and share a sequence identity of 85%.

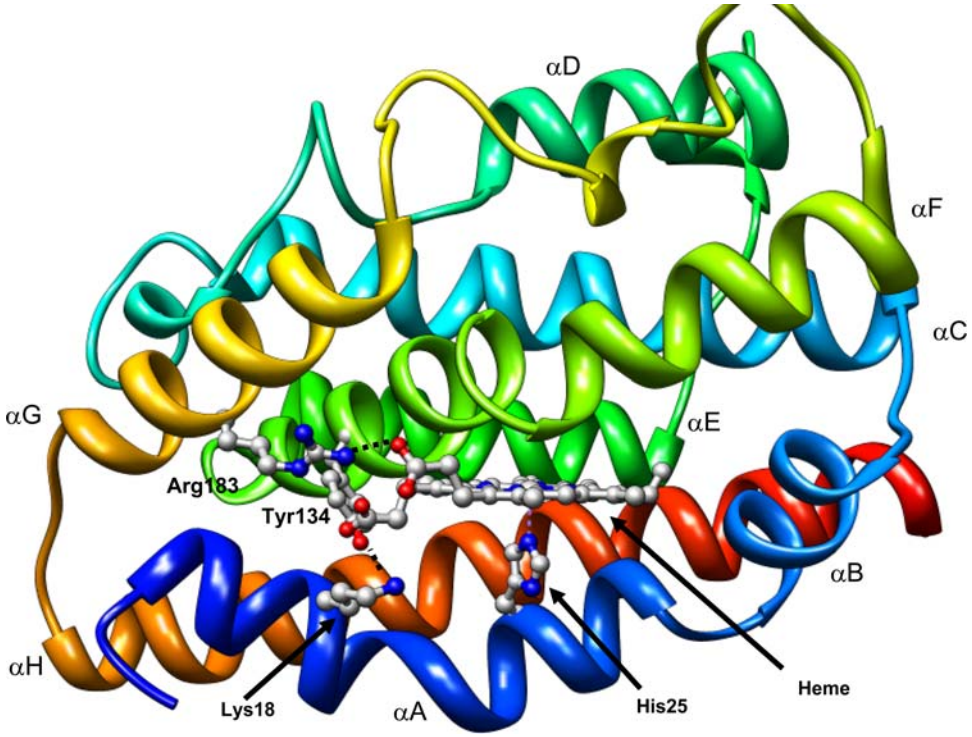

Fig. 1 General structure of mammalian heme oxygenase 1. The backbone is represented in ribbon and the important residues in the heme-binding site and the heme group in ball and stick. Example taken from the rat species

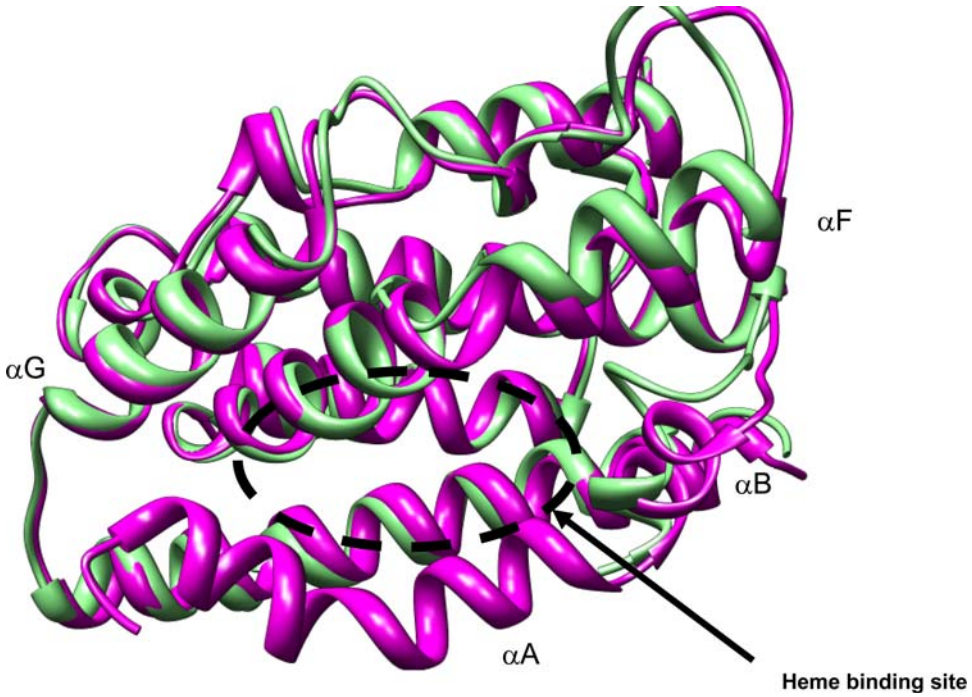

Fig. 2 Overlap between the rat apo (*clear green*) and human apo (*dark purple*) heme oxygenases 1. The heme-binding site and its closest helices are highlighted. Note the missing N-terminal part in the former

A closer inspection of the structures shows that at least two helices are involved in the conformational transition between open and closed form. On the one side, the B helix switches from a position out of the binding site in the open conformation to a position inside the binding site in the closed conformation. Correlated to this movement is the bending of the F helix which displaces part of the helix further from the heme in the closed form than in the open one (note here that we refer to "open" and "closed" conformations taking into account the relative position of the B helix with respect to the binding site). Unfortunately, the transition described by these two structures cannot well be understood since in the crystallographic form of the closed structure; the helix A is completely missing. The importance of this helix in the mechanism of the binding of the heme raises therefore different questions on the exact

structural variables involved for stabilizing one of the two conformations: what is the overall conformation of the complete closed form of the rat heme-free HO-1? What is the possible involvement of the A-helix into the transition between open and closed forms? Is the heme-free rat HO-1 actually able to adopt the same open structure as the human one? What is the general mechanism for the transition between the two structures? And why those experimentally characterized structures are in different conformational states? Because the transition between the two structures are mainly involving the entire scaffold of the protein and that the missing part of the closed form is a large region of the tertiary structure, exploration of the low energy motions could provide sufficient amount of information for accurate structural modeling.

Here, we present an original approach based on full-atom NMA to generate complete structural models of heme-free forms of the rat HO-1. Starting from an initial minimized structure of a rat heme-bound form where we removed the heme, we displaced the structure following the lowest frequency modes toward the X-ray structures of apo proteins. In doing so, we generated a set of 3D models of the rat HO-1 with forms as close as possible to (1) the heme-free human HO-1 structure and (2) the heme-free rat HO-1 one. In the latter case, our displaced structure contains the A helix entirely. To evaluate how close both displaced structures are to the structures of the corresponding templates we computed the root mean square differences of atomic positions (rms) between the respective structures.

Material and methods

Energy minimization and NMA

The initial structure considered in this work corresponds to one of the X-ray structures available for the rat heme-bound HO-1 [code PDB 1dve (Sugishima et al. 2000)]. This structure was first minimized after removal of the prosthetic group. The force field used is the one corresponding to the parameter set 22 of the CHARMM program (Brooks et al. 1983). The electrostatic interactions were computed with a $2r$ dependent dielectric constant, r being the distance between the interacting atoms. The switch function was used for the Van der Waals interactions, and a shift function for the electrostatic interactions. The cuton and cutoff values used were 10 and 12 Å, respectively. The energy minimization was carried out by performing 10,000 steps of conjugate gradient method followed by the ABNR (adopted basis Newton Raphson) method up to a mean energy gradient of 10^{-5} kcal/mol/Å. Such a low gradient is required for computing the normal modes in the full-atom representation. The first 500 lowest frequency modes of this minimized structure were computed by using the DIMB method (Perahia and Mouawad 1995) up to a convergence of 0.06 for the eigenvectors.

Displacement along the modes with best-fit algorithm

The energy minimized structure was initially superimposed to one of the template structures (closed or open form). The atoms of the target were then displaced along the first lowest frequency eigenvector until reaching a minimum value for the rms difference with respect to the template considered. This was achieved by generating a grid of points corresponding to the structures displaced along the eigenvector in both directions and with a spacing between successive points of 0.05 Å of rms variations. This structure was in turn displaced along the second lowest frequency mode to reach a new minimum for the rms difference with respect to the template. This procedure was repeated until all the successive modes ordered in increasing frequencies were considered for the displacements. Note that there is a cumulative structural change over the multiple modes. We found that the ordering of modes for the displacements has a very minor effect on the final structure obtained.

Results and discussion

The main objective of this study is to use NMA-based approaches to generate *complete* structures of the *rat* heme-free HO-1 in both *open* and *closed* forms. The general approach of this study is presented in Fig. 3.

Since no complete apo structure of rat is HO-1 is available in the Protein Data Bank (only an incomplete structure of the rat heme-free form exists), the initial structure considered to initiate our work was the one generated from a heme-bound structure of rat HO-1 (pdb code 1dve) (Sugishima et al. 2000) from which the prosthetic group was removed. To carry out the NMA calculations in the full-atom force field, this structure was first minimized. Since no explicit solvent molecules were considered, the resulting minimized structure has obviously a more compact structure and presents structural deviations with all the other HO-1 mammalian experimental structures reaching rms differences as large as 1.7 Å. However, the general fold of the protein is not altered at all. Because the lowest frequency modes depend to a large part on the topology of the molecule, the structural changes due to the minimization process should not modify importantly the general motions of the protein. With respect to the structural templates, this energy minimized structure presents rms deviations of 1.7 and 1.5 Å with respect to the open and the closed form of the heme-free HO-1, respectively. These deviations are slightly larger than those generally observed between the

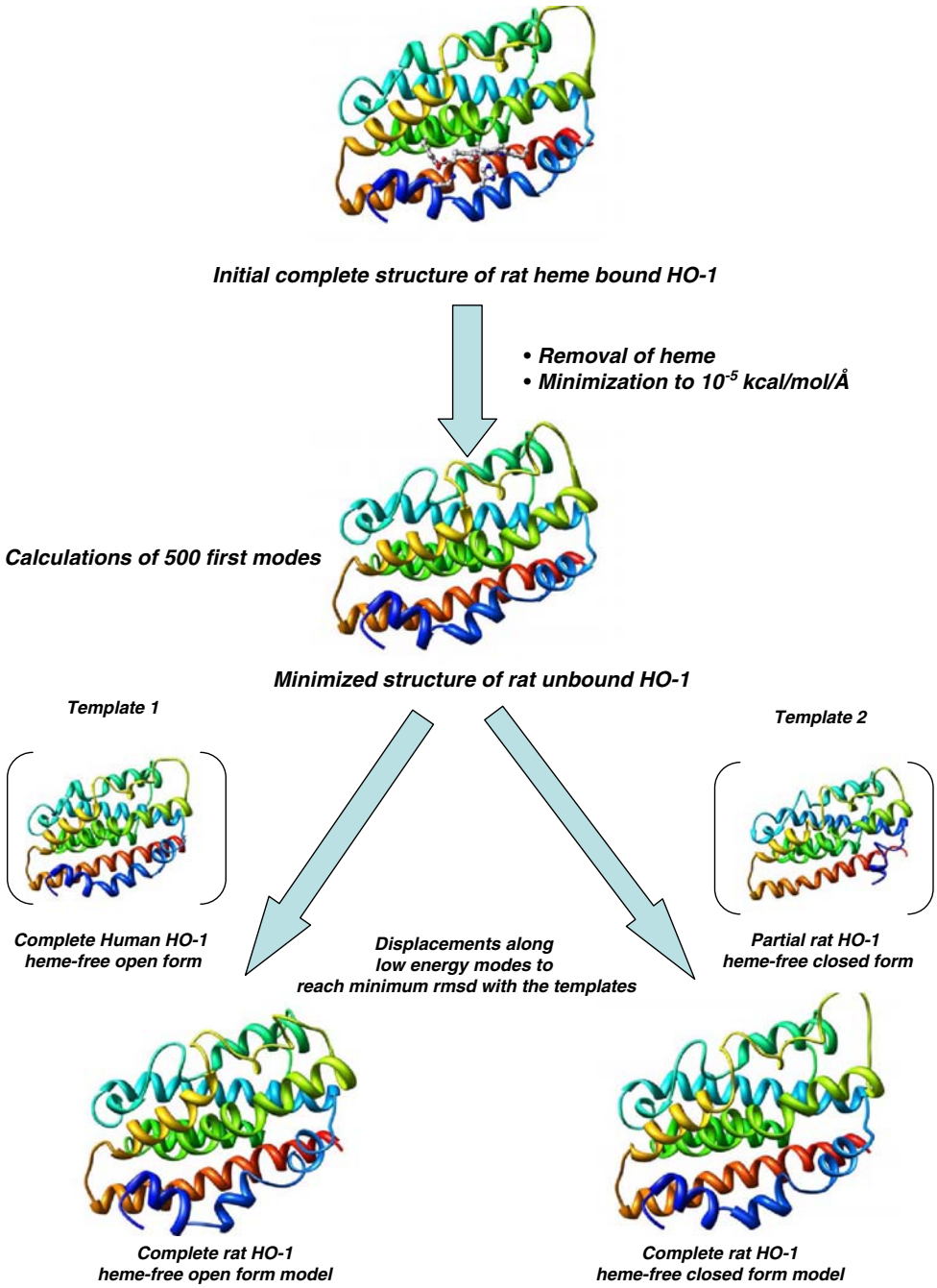

Fig. 3 General procedure undertaken for the generation of open and closed models of the rat heme oxygenase-1

different experimental HO-1 structures which generally range from 0.4 to 1.2 Å approximately. As we will see later on, the displacements along the modes will result to a substantial decrease of rms values.

Successive displacements along the low energy modes toward the two structural templates were performed using the best-fit algorithm. In a first instance, all the modes with frequencies lower than 70 cm^{-1} have been selected for these displacements (approximately 500 modes). The successive displacements carried out on normal modes from the lowest frequency modes to the higher ones show that the resulting displaced structures get rapidly closer to the structure of the templates considered (Fig. 4a). The rms values decrease from 1.6 to 0.5 Å for the human and from 1.4 to 0.6 Å for the rat form after 500 modes displacements. This time, those values are in the range of rms values observed between the experimental structures.

Two additional interesting observations result from this part of the study. On the one side, the analysis of the percentage of displacement toward the structural templates shows that in both cases almost 80% of the overall possible displacement is obtained with only 100 modes (Fig. 4b).

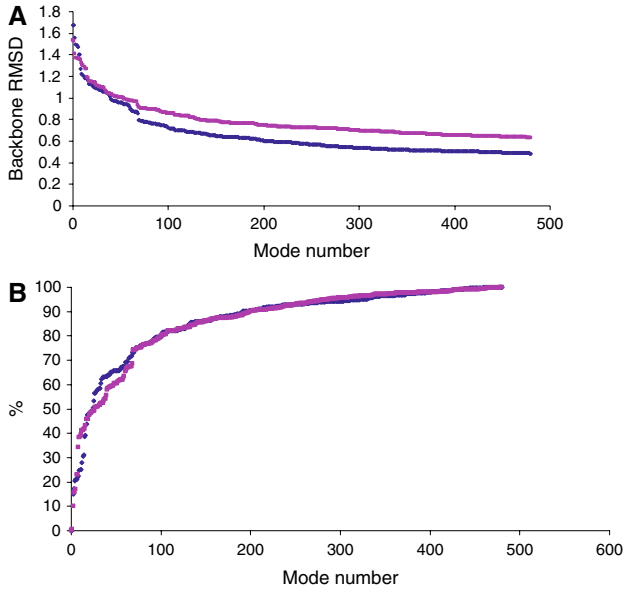

Fig. 4 **a** The rms deviations between displaced structures and the open (*light purple*) and the closed (*dark blue*) templates. **b** Percentage of contribution of modes regarding the maximum possible displacement. In this figure, the modes are numbered in the order of increasing frequencies

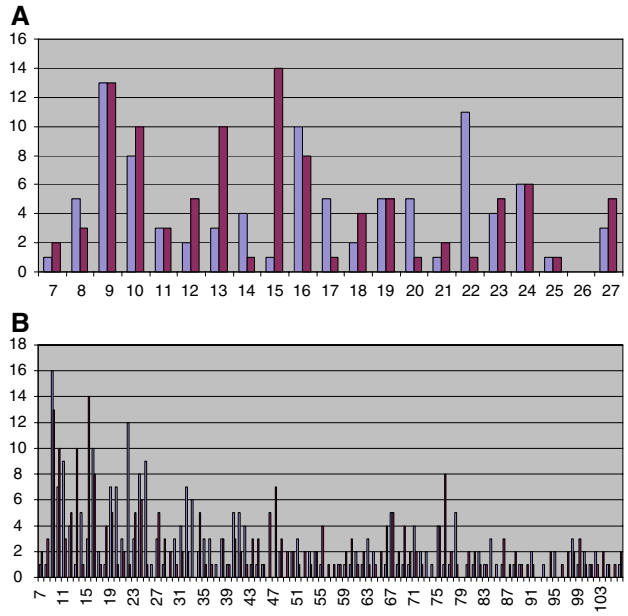

Fig. 5 Individual contributions of normal modes to displacements toward open (*dark purple*) and closed (*light blue*) templates. The height of the *bars* corresponds to the number of steps performed along a given mode. The different panels correspond to **a** the 20 first normal modes and **b** the 100 first normal modes

No significant improvement is observed for the remaining modes. This highlights therefore that the lowest 100 modes should suffice to provide heme-free rat HO-1 models of good structural quality. On the other side, the same analysis also shows that the exploration on only few modes like the 5 or 10 lowest frequency ones provide displacements which account to less than 20% of the global displacement. This result differs from the general application of NMA, where only the very lowest modes are investigated. One of the explanations for this observation is that the HO-1 is a small protein and does not present clear domain motions for which the very few lowest modes can be already enough for exploring the motions of the protein. Another reason is the extensive minimization that was performed and that compacted the structure resulting in a shift of vibrational frequencies to higher values and consequently the contribution of normal modes to conformational changes is of lower magnitudes. A more detailed observation of the rms variations shows also that they slightly differ depending on the structure we try to match.

The individual contributions to the global displacement of each mode were analyzed for the first 100 modes (Fig. 5a, b). For the very low frequency modes (from mode 7 to mode 12), the numbers of favorable steps to get closer to the templates are almost the same for both open and closed conformations. Beyond that, behaviors are slightly different depending on the structural templates selected. Until the 30th mode, getting closer to the open structure requires major displacements on modes 13 and 15 while getting closer to the closed form requires major displacements on modes 16, 17, 20 and 22. For upper frequencies, fewer modes are involved for important structural transitions. Some isolated peaks show although that the profile of the displacements toward the open and closed structures remains different (Fig. 5b), e.g., mode 77 for the open structure and 79 for the closed one. The directions of motions corresponding to modes 13, 15 and 22 leading to open and closed structures are shown in Fig. 6. Although these modes involve mainly the same regions of the protein (heme-binding site and helices A, B and F), their directions are quite different. In modes 13 and 15, the B helix mainly moves away from the binding-site cavity while in mode 22 it moves closer by rotation around its center of mass blocking the entrance of the binding site. The A helix also behaves differently depending on the mode of interest, while accompanying the general motion of the B helix, its motion is quite substantial in the modes 13 and 15 but not in the mode 22. It appears therefore that different low energy conformational paths are involved leading from the open heme-bound form toward heme-free open and closed forms.

We analyze here in more details the models built by using the best-fit algorithm. In order to correct the structural distortions arising from NMA displacements and refine the inter-residue interactions the models were energy minimized. As expected a similar trend is observed for the rms variations of the energy minimized structures comparatively

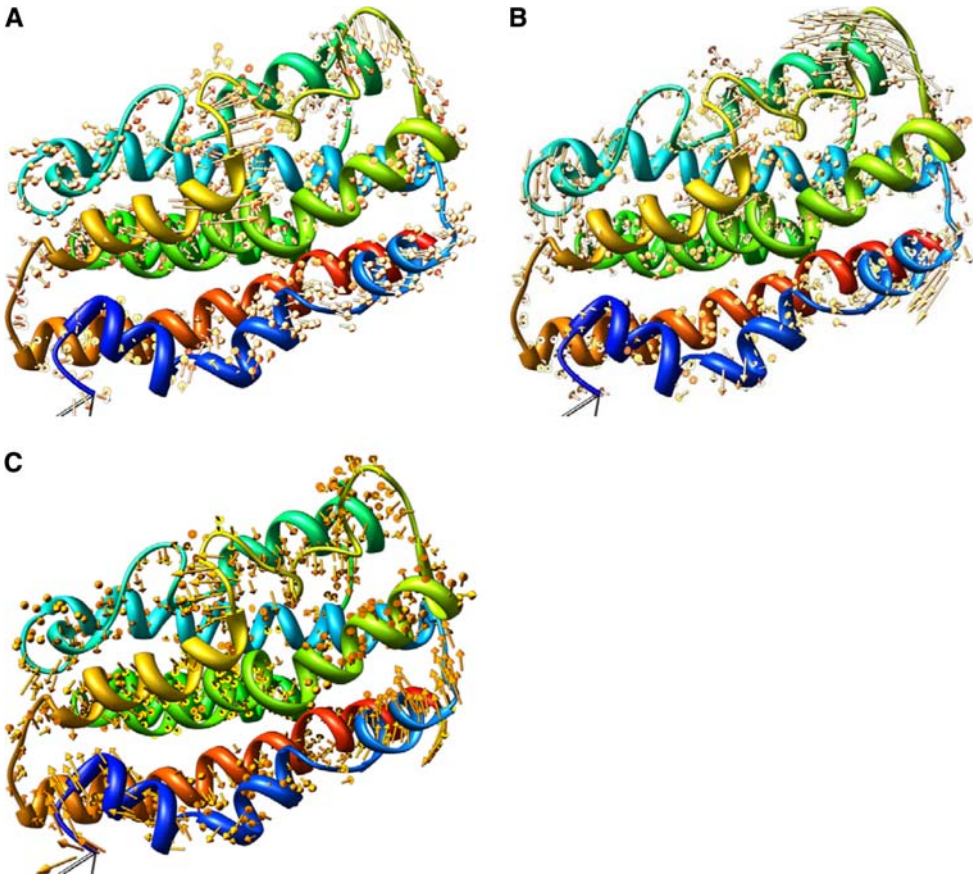

Fig. 6 Representation of the normal modes involved in the construction of either open or closed models. **a** Modes 13, **b** mode 15, **c** mode 22

to simply displaced structures. The rms variations of the minimized structures are presented in Table 1. For the structures displaced toward the open conformation, one can see that substantial variations exist between the structures obtained after successive displacements on 5 and 10 modes. The rms value drops from 1.8 to 1.2 Å. This is explained by the important contribution of modes 13 and 15 in the transition from the initial structure to the open form. Structures generated after 20 and 50 modes also present appreciable decrease of the rms relative to the open conformation. For 100 modes the rms deviation is about 0.7 Å. Interestingly, the main differences between the different structures concern the part of the protein corresponding to the overall heme-binding pocket. In particular, one can see (Fig. 6) how the helix A gets further from the rest of the protein core. For the structures obtained after displacements toward the closed conformation, the general trend of the rms variations is similar to the one observed for the open one (Table 1). Here also the rms values drop from 1.6 to 0.8 Å for 100 modes.

Table 1 The rms values between the template and the minimized structures after displacement along a given number of normal modes and corresponding to the energy differences with respect to the energy minimized structure for which the normal modes were computed

	Number of modes	RMSD deviation against template	ΔE with minimized structure (kcal/mol)
Open conformation	0	1.8	0.0
	5	1.5	−0.6
	10	1.2	17.4
	20	1.1	22.0
	50	1.0	11.8
	100	0.7	29.9
Closed conformation	0	1.6	0.0
	5	1.4	−0.75
	10	1.3	10.64
	20	1.1	−2.8
	50	1.0	4.4
	100	0.8	−5.82

The analysis of the differences in potential energy between the conformations generated by displacements along the modes was performed. As one can see in Table 1, the energy of the structures does not exceed 30 kcal/mol with respect to the one initially minimized to compute the modes. Interestingly, different tendencies are observed when the displacements take place toward the open conformation or the closed one. When displacing the structure toward the open conformation, the energy difference tends to increase as the number of modes increases. Only the

structure generated along 50 modes escapes this tendency (+11.8 kcal/mol). This is attributed to the participation of several modes between 20 and 50 having particular structural relevance. When displacements are performed toward the closed conformation, the energy differences do not exceed 11 kcal/mol and the general energetic pattern is not correlated with the number of modes. While displacements over 10 modes lead to an increase of the energy of approximately 10 kcal/mol, the structure generated after displacements over 100 modes leads to a stabilization of 5.8 kcal/mol with respect of the initial structure. Two major points arise from these energetic considerations. On the one hand, the alternative conformations of rat HO-1 generated along the lowest frequency normal modes appear mainly stable even when 100 modes are considered. On the other hand, the rat HO-1 close-like structures are substantially more stable than the open-like ones. This is therefore consistent with the experimental observations showing that the crystal structure of the rat HO-1 exhibits a closed-like form. Obviously, only free-energy calculations would provide an accurate estimation of the energetic profiles of the conformational transitions between the different conformations of the enzymes. Such calculations are now in progress. However, the structural models generated in this work allow us to discuss on the origin of the stability of the different types of conformations of the rat HO-1.

The NMA modeling of the two complete heme-free models of the rat HO-1 provided us with the possibility for getting a deeper insight into the structural characteristics of the two open and closed forms. Most of the structural differences between the two forms of rat HO-1 are located in the binding site heme region and involve helices A, B and F. While the open structure reveals a quite open heme-binding site cavity, the entrance of this site is blocked in the closed structure by the positioning of the A helix near the F-helix, forming between them a hydrogen bond involving the residues His25 and Tyr134 (Fig. 7). It is important to note that both residues are involved in the polar interactions observed in the fixation of the prosthetic group; His25 is involved in the coordination bond with the iron atom and Tyr134 interacts with one of the propionates of the heme to stabilize its position in the active site (see Fig. 1). Moreover, in the open conformation these two residues are quite distant (distance between the oxygen of the side chain of Tyr134 and N_{ε} of the His25 is about 10 Å). Among the different structural factors that can stabilize the open form against the closed one of the rat HO-1, we can mention the implication of Glu29. This residue forms a strong hydrogen bond with His25 in the open form, which has mainly an ionic character, while in the closed form the residue His25 form a weaker hydrogen bond with Tyr134. Such a situation could point to the possibility for the open structure to be more favored than the closed one.

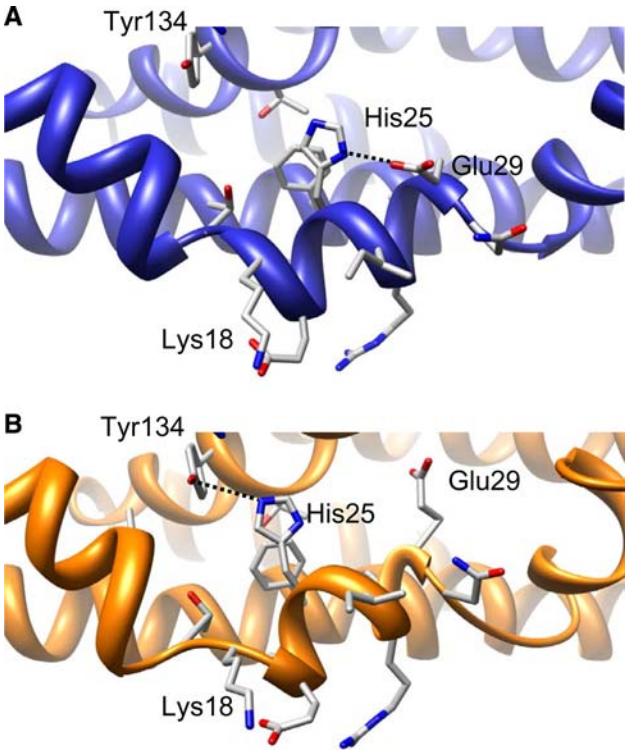

Fig. 7 Interactions between key residues of the A, B and F helices for the rat free-heme open (**a**) and free-heme closed (**b**) energy minimized structures

Conclusion

We show in this article how to build heme-free 3D models of the rat HO-1 using normal modes computed for a unique structure and guided by different templates of homologous structures, one of them having missing parts in key physiological regions. The structural best-fit algorithm based on normal modes displacements that we presented here provides an improved way for taking into account the conformational flexibility of the backbone scaffold of the target, and represents therefore an interesting add-on for the general framework of homology modeling. Moreover, the 3D models of the rat HO-1 that this approach allowed us to build were useful to get substantial insight into the stabilizing factors of the open and closed forms, and to characterize the collective motions which lead from one form to the other. Obviously, the protein structures we obtained here represent still a limited structural choice, and further analysis may be required, like molecular dynamics simulations, to better investigate the conformational preferences and the transitions between the different forms. However, this first approach already provided interesting structural information missing from actual experimental knowledge.

References

Brooks B, Bruccoleri R, Olafson B, States D, Swaminathan S, Karplus M (1983) Charmm: a program for macromolecular energy, minimization, and dynamics calculations. J Comput Chem 4:187–217

Brooks BR, Janežič D, Karplus M (1995) Harmonic analysis of large systems. I: Methodology. J Comput Chem 16:1522–1542

Cavasotto C, Kovacs J, Abagyan RA (2005) Representing receptor flexibility in ligand docking through relevant normal modes. J Am Chem Soc 127:9632–9640

Chen X, Poon B, Dousis A, Wang Q, Ma J (2007) Normal-mode refinement of anisotropic thermal parameters for potassium channel KcsA at 3.2 Å crystallographic resolution. Structure 15:955–962

Cui Q, Bahar I (2006) Normal mode analysis: theory and applications to biological and chemical systems. Chapman & Hall, London

Cui Q, Li G, Ma J, Karplus M (2004) A normal mode analysis of structural plasticity in the biomolecular motor F1-ATPase. J Mol Biol 340:345–372

Eyal E, Yang L-W, Bahar I (2006) Anisotropic network model: systematic evaluation and a new web interface. Bioinformatics 22:2619–2627

Eswar N, John B, Mirkovic N, Fiser A, Ilyin V, Pieper U, Stuart A, Marti-Renom M, Madhusudhan M, Yerkovich B, Sali A (2003) Tools for comparative protein structure modeling and analysis Nucl. Acids Res 31:3375–3380

Fiser A, Sali A (2003) ModLoop: automated modeling of loops in protein structures. Bioinformatics 19:2500–2501

Floquet N, Maréchal J-D, Badet-Denisot M-A, Robert C, Dauchez M, Perahia D (2006) Normal mode analysis as a prerequisite for drug design: application to matrix metalloproteinases inhibitors. FEBS Lett 580:5130–5136

Guilbert C, Pecorari F, Perahia D, Mouawad L (1996) Low frequency motions in phosphoglycerate kinase: a normal mode analysis. Chem Phys 204:327–336

Krieger E, Sander B, Vriend G (2003) Homology modeling. In: Bourne P, Weissig H (eds) Structural bioinformatics, vol 44. Wiley–Liss, New York, pp 507–521

Lad L, Schuller D, Shimizu H, Friedman J, Li H, Ortiz de Montellano P, Poulos T (2003) Comparison of the heme-free and -bound crystal structures of human heme oxygenase-1. J Biol Chem 278:7834–7843

Leo-Macias A, Lopez-Romero P, Lupyan D, Zerbino D, Ortiz AR (2005) Core deformations in protein families: a physical perspective. Biophys Chem 115:125–128

Li G, Cui Q (2002) A coarse-grained normal mode approach for macromolecules: an efficient implementation and application to Ca2þ -ATPase. Biophys J 83:2457–2474

May A, Zacharias M (2005) Accounting for global protein deformability during protein–protein and protein–ligand docking. Biochim Biophys Acta 1754:225–231

Mouawad L, Perahia D (1996) Motions in haemoglobin studied by normal mode analysis and energy minimization. Evidence for the existence of tertiary T-like, quaternary R-like intermediate structures. J Mol Biol 258:393–410

Perahia D, Mouawad L (1995) Computation of low frequency normal modes in macromolecules: improvements to the method of diagonalization in a mixed basis and application. Comput Chem 19:241–246

Sugishima M, Omata Y, Kakuta Y, Sakamoto H, Noguchi M, Fukuyama K (2000) Crystal structure of rat heme oxygenase-1 in complex with heme. FEBS Lett 471:61–66

Sugishima M, Sakamoto H, Kakuta Y, Omata Y, Hayashi S, Noguchi M, Fukuyama K (2002) Crystal structure of rat apo-heme oxygenase-1 (HO-1): mechanism of heme binding in HO-1 inferred from structural comparison of the apo and heme complex forms. Biochemistry 41:7293–7300

Tama F, Gadea F, Marques O, Sanejouand Y (2000) Building-block approach for determining low-frequency normal modes of macromolecules. Proteins Struct Funct Genet 41:1

Tama F, Miyashita O, Brooks C (2004) Normal mode based flexible fitting of high-resolution structure into low-resolution experimental data from cryo-EM. J Struct Biol 147:315–326

Thomas A, Field M, Mouawad L, Perahia D (1996) Analysis of the low frequency normal modes of the T-state of Aspartate transcarbamylase. J Mol Biol 257:1070–1087

Wu Y, Tian X, Lu M, Chen M, Wang Q, Ma J (2005) Folding of small helical proteins assisted by small-angle X-ray scattering profiles. Structure 13:1587–1597